Four-wave mixing signal enhancement and optical bistability of a hybrid metal nanoparticle-quantum dot molecule in a nanomechanical resonator

Jian-Bo Li,[1,*] Shan Liang,[2] Si Xiao,[3] Meng-Dong He,[1] Nam-Chol Kim,[4] Li-Qun Chen,[1] Gui-Hong Wu,[1] Yu-Xiang Peng,[1] Xiao-Yu Luo,[1] and Ze-Ping Guo[1]

[1]*Institute of Mathematics and Physics, Central South University of Forestry and Technology, Changsha, 410004, China*

[2]*Department of Physics, Hunan Normal University, Changsha, 410081, China*

[3]*School of Physics and Electronics, Hunan Key Laboratory for Super-microstructure and Ultrafast Process, Central South University, Changsha, 410083, China*

[4]*Department of Physics, Kim Il Sung University, Pyongyang, North Korea*

[*]*jbli_opt@csuft.edu.cn*

Abstract: We investigate theoretically four-wave mixing (FWM) response and optical bistability (OB) in a hybrid nanosystem composed of a metal nanoparticle (MNP) and a semiconductor quantum dot (SQD) coupled to a nanomechanical resonator (NR). It is shown that the FWM signal is enhanced by more than three orders of magnitude as compared to that of the system without exciton-phonon interaction, and the FWM signal can also be suppressed significantly and broadened due to the exciton-plasmon interaction. As the MNP couples strongly with the SQD, the bistable FWM response can be achieved by adjusting the SQD-MNP distance and the pumping intensity. For a given pumping constant and a fixed SQD-MNP distance, the enhanced exciton-phonon interaction can promote the occurrence of bistability. Our findings not only present a feasible way to detect the spacing between two nanoparticles, but also hold promise for developing quantum switches and nanoscale rulers.

OCIS codes: (190.4380) Nonlinear optics, four-wave mixing; (190.1450) Bistability; (160.4236) Nanomaterials; (240.6680) Surface plasmons.

References and links

1. S. Kühn, U. Håkanson, L. Rogobete, and V. Sandoghdar, "Enhancement of single-molecule fluorescence using a gold nanoparticle as an optical nanoantenna," Phys. Rev. Lett. **97**(1), 017402 (2006).
2. H. M. Gong, X. H. Wang, Y. M. Du, and Q. Q. Wang, "Optical nonlinear absorption and refraction of CdS and CdS-Ag core-shell quantum dots," J. Chem. Phys. **125**(2), 024707 (2006).
3. J. Y. Yan, W. Zhang, S. Duan, X. G. Zhao, and A. O. Govorov, "Optical properties of coupled metal-semiconductor and metal-molecule nanocrystal complexes: Role of multipole effects," Phys. Rev. B **77**(16), 165301 (2008).
4. D. C. Marinica, A. K. Kazansky, P. Nordlander, J. Aizpurua, and A. G. Borisov, "Quantum plasmonics: Nonlinear effects in the field enhancement of a plasmonic nanoparticle dimer," Nano Lett. **12**(3), 1333–1339 (2012).
5. S. G. Kosionis, A. F. Terzis, S. M. Sadeghi, and E. Paspalakis, "Optical response of a quantum dot-metal nanoparticle hybrid interacting with a weak probe field," J. Phys. Condens. Matter **25**(4), 045304 (2013).
6. S. M. Sadeghi, "Optical routing and switching of energy flow in nanostructure systems," Appl. Phys. Lett. **99**(11), 113113 (2011).
7. W. Zhang, A. O. Govorov, and G. W. Bryant, "Semiconductor-metal nanoparticle molecules: hybrid excitons and the nonlinear Fano effect," Phys. Rev. Lett. **97**(14), 146804 (2006).
8. X. B. Feng, G. C. Xing, and W. Ji, "Two-photon-enhanced three-photon absorption in transition-metal-doped semiconductor quantum dots," J. Opt. A, Pure Appl. Opt. **11**(2), 024004 (2009).
9. J. Zhang, Y. Tang, K. Lee, and M. Ouyang, "Tailoring light-matter-spin interactions in colloidal hetero-nanostructures," Nature **466**(7302), 91–95 (2010).
10. M. R. Singh, "Enhancement of the second-harmonic generation in a quantum dot-metallic nanoparticle hybrid system," Nanotechnology **24**(12), 125701 (2013).

#253917 Received 16 Nov 2015; revised 19 Jan 2016; accepted 22 Jan 2016; published 29 Jan 2016

11. D. Turkpence, G. B. Akguc, A. Bek, and M. E. Tasgin, "Engineering nonlinear response of nanomaterials using Fano resonances," J. Opt. **16**(10), 105009 (2014).
12. W. X. Yang, A. X. Chen, Z. Huang, and R. K. Lee, "Ultrafast optical switching in quantum dot-metallic nanoparticle hybrid systems," Opt. Express **23**(10), 13032–13040 (2015).
13. J. B. Li, N. C. Kim, M. T. Cheng, L. Zhou, Z. H. Hao, and Q. Q. Wang, "Optical bistability and nonlinearity of coherently coupled exciton-plasmon systems," Opt. Express **20**(2), 1856–1861 (2012).
14. A. V. Malyshev and V. A. Malyshev, "Optical bistability and hysteresis of a hybrid metal-semiconductor nanodimer," Phys. Rev. B **84**(3), 035314 (2011).
15. R. D. Artuso and G. W. Bryant, "Optical response of strongly coupled quantum dot-metal nanoparticle systems: double peaked Fano structure and bistability," Nano Lett. **8**(7), 2106–2111 (2008).
16. H. I. Elim, W. Ji, J. Yang, and J. Y. Lee, "Intensity-dependent enhancement of saturable absorption in PbS -Au_4 nanohybrid composites: Evidence for resonant energy transfer by Auger recombination," Appl. Phys. Lett. **92**(25), 251106 (2008).
17. M. T. Cheng, S. D. Liu, and Q. Q. Wang, "Modulating emission polarization of semiconductor quantum dots through surface plasmon of metal nanorod," Appl. Phys. Lett. **92**(16), 162107 (2008).
18. C. H. R. Ooi and K. S. Tan, "Controlling double quantum coherence and electromagnetic induced transparency with plasmonic metallic nanoparticle," Plasmonics **8**(2), 891–898 (2013).
19. Z. H. Xiao, L. Zheng, and H. Lin, "Photoinduced diffraction grating in hybrid artificial molecule," Opt. Express **20**(2), 1219–1229 (2012).
20. S. M. Sadeghi and K. D. Patty, "Suppression of quantum decoherence via infrared-driven coherent exciton-plasmon coupling: Undamped field and Rabi oscillations," Appl. Phys. Lett. **104**(8), 083101 (2014).
21. S. Palomba and L. Novotny, "Nonlinear excitation of surface plasmon polaritons by four-wave mixing," Phys. Rev. Lett. **101**(5), 056802 (2008).
22. J. Renger, R. Quidant, N. van Hulst, and L. Novotny, "Surface-enhanced nonlinear four-wave mixing," Phys. Rev. Lett. **104**(4), 046803 (2010).
23. M. Kauranen and A. V. Zayats, "Nonlinear plasmonics," Nat. Photonics **6**(11), 737–748 (2012).
24. Z. E. Lu and K. D. Zhu, "Enhancing Kerr nonlinearity of a strong coupled exciton-plasmon in hybrid nanocrystal molecules," J. Phys. B **41**(18), 185503 (2008).
25. M. Danckwerts and L. Novotny, "Optical frequency mixing at coupled gold nanoparticles," Phys. Rev. Lett. **98**(2), 026104 (2007).
26. E. Paspalakis, S. Evangelou, S. G. Kosionis, and A. F. Terzis, "Strongly modified four-wave mixing in a coupled semiconductor quantum dot-metal nanoparticle system," J. Appl. Phys. **115**(8), 083106 (2014).
27. X. N. Liu, D. Z. Yao, H. M. Zhou, F. Chen, and G. G. Xiong, "Third-order nonlinear optical response in quantum dot-metal nanoparticle hybrid structures," Appl. Phys. B **113**(4), 603–610 (2013).
28. J. B. Li, M. D. He, and L. Q. Chen, "Four-wave parametric amplification in semiconductor quantum dot-metallic nanoparticle hybrid molecules," Opt. Express **22**(20), 24734–24741 (2014).
29. K. L. Ekinci, "Electromechanical transducers at the nanoscale: actuation and sensing of motion in nanoelectromechanical systems (NEMS)," Small **1**(8-9), 786–797 (2005).
30. H. Wang and K. D. Zhu, "Coherent optical spectroscopy of a hybrid nanocrystal complex embedded in a nanomechanical resonator," Opt. Express **18**(15), 16175–16182 (2010).
31. J. J. Li and K. D. Zhu, "Plasmon-assisted mass sensing in a hybrid nanocrystal coupled to a nanomechanical resonator," Phys. Rev. B **83**(24), 245421 (2011).
32. M. Ringler, A. Schwemer, M. Wunderlich, A. Nichtl, K. Kürzinger, T. A. Klar, and J. Feldmann, "Shaping emission spectra of fluorescent molecules with single plasmonic nanoresonators," Phys. Rev. Lett. **100**(20), 203002 (2008).
33. O. Hess, J. B. Pendry, S. A. Maier, R. F. Oulton, J. M. Hamm, and K. L. Tsakmakidis, "Active nanoplasmonic metamaterials," Nat. Mater. **11**(7), 573–584 (2012).
34. T. Kalkbrenner, U. Håkanson, and V. Sandoghdar, "Tomographic plasmon spectroscopy of a single gold nanoparticle," Nano Lett. **4**(12), 2309–2314 (2004).
35. I. Wilson-Rae, P. Zoller, and A. Imamoğlu, "Laser cooling of a nanomechanical resonator mode to its quantum ground state," Phys. Rev. Lett. **92**(7), 075507 (2004).
36. C. F. Bohren and D. R. Huffman, *Absorption and Scattering of Light by Small Particles* (Wiley, 1983).
37. V. V. Batygin and I. N. Toptygin, *Sbornik Zadach Po Elektrodinamike* 2-e izd. (M.: Nauka, 1970); *Problems In Electrodynamics*, 2nd ed. (Academic Press, 1978).
38. E. D. Palik, *Handbook of Optical Constants of Solids* (Academic Press, 1985).
39. R. W. Boyd, *Nonlinear Optics*, 3nd ed (Academic Press, 2008).
40. W. Ni, T. Ambjörnsson, S. P. Apell, H. Chen, and J. Wang, "Observing plasmonic-molecular resonance coupling on single gold nanorods," Nano Lett. **10**(1), 77–84 (2010).
41. M. G. Benedict, V. A. Malyshev, E. D. Trifonov, and A. I. Zaitsev, "Reflection and transmission of ultrashort light pulses through a thin resonant medium: Local-field effects," Phys. Rev. A **43**(7), 3845–3853 (1991).

1. Introduction

Significant research efforts are now being devoted toward the investigation of the impact of exciton-plasmon interaction on the optical properties of metal-semiconductor hybrid nanosystems [1–6]. Recent studies have shown that the exciton-plasmon interaction can drastically modify the optical properties of metal-semiconductor hybrid nanosystems, such as

#253917 Received 16 Nov 2015; revised 19 Jan 2016; accepted 22 Jan 2016; published 29 Jan 2016

nonlinear Fano effect [7], two-photon-enhanced three-photon absorption [8], optical Stark effect [9], second harmonic generation [10,11], ultrafast excitonic population inversion [12], optical bistability [13–15]and intensity-dependent enhancement of saturable absorption [16]. Moreover, strong exciton-plasmon interaction allows us to modulate emission polarization of semiconductor quantum dots (SQDs) [17], control electromagnetically induced transparency [18], improve the diffraction efficiency of the grating [19], and suppress quantum decoherence [20].

Four-wave mixing (FWM) response, as an exciting nonlinear optical phenomenon, has been extensively studied in the same complex nanostructures. It is reported that optical FWM can be used to excite surface plasmon polaritons on a metal film [21], and surface plasmon polaritons can be used to enhance the FWM as well [22,23]. Based on plasmonic effects, the FWM response of the nanosystem can be effectively modified. Recently, Zhu et al. demonstrated that the FWM response in a coupled SQD-metal nanoparticle (MNP) system can be enhanced greatly arising from the exciton-plasmon interaction [24]. That is quite different from the FWM enhancement in the gold nanoparticles nanosystem [25]. Paspalakis et al. obtained single-peaked and three-peaked FWM spectra by adjusting the spacing between the MNP and the SQD [26]. Xiong et al. reported that the FWM response of the SQD coupled to the MNP can be enhanced remarkably by changing the geometrical parameters of the system and the polarized direction of the electric field [27]. Li et al. showed that highly efficient four-wave parametric amplification can be achieved by adjusting the frequency and the intensity of the pump field and the distance between the SQD and the MNP [28].

Besides, another interesting nanostructural material is the nanomechanical resonator (NR), which holds promise for scientific and technical applications because of its environment, high-Q factor and small size [29]. Some NR-based nanosystems can be used to explore nonlinear optical and quantum effects [30–33]. When a hybrid SQD-MNP complex embedded in a NR was subjected by a weak pump field, the accreted mass landing on the NR can be measured according to the frequency shift in the probe nonlinear absorption spectrum [31]. However, the FWM response of the MNP-SQD-NR system in a strong pump field modulated by the exciton-phonon interaction and the exciton-plasmon interaction was never further explored. In this paper, we study the FWM response of the MNP-SQD-NR system arised from two interactions. We show that the FWM signal can be enhanced dramatically due to the exciton-phonon interaction, and such signal can also be suppressed significantly and broadened arising from the exciton-plasmon interaction. Moreover, we reveal that the FWM signal exhibits bistable properties by modulating the SQD-MNP distance and the pumping intensity. We also address that, for a given pumping constant and a fixed nanostructure, the enhanced exciton-phonon interaction can promote the occurrence of bistability.

2. Model and formalism

We consider a nanosystem consisting of a MNP of radius a and a SQD of radius r coupled to a NR. The center-to-center distance between the MNP and the SQD is d, as shown in Fig. 1(a). The nanosystem is subjected to a strong pump field and a weak probe field. E_{pu} (E_{pr}) is the amplitude of the pump field (probe field), and ω_{pu} (ω_{pr}) is the frequency of the pump field (probe field). The MNP is fixed to an optical fiber tip, which can be moved and stabilized by using an atomic force microscope (AFM) [34]. It is necessary to point out that the optical fiber tip is only used as an auxiliary component in our system, so we neglect the effect of the tip to the system. By choosing the direction of the pump field to be either perpendicular or parallel to the axis of the hybrid system, we in turn only excite one of the three excitons in the SQD [15]. In these cases, the SQD can be treated as a two-level system consisting of a ground state (no exciton) $|0\rangle$ and the first excited state (single exciton) $|1\rangle$, which is characterized by the pseudospin operators σ_{01}, σ_{10} and σ^{z}. The physical situation is illustrated in Fig. 1(b).

#253917 Received 16 Nov 2015; revised 19 Jan 2016; accepted 22 Jan 2016; published 29 Jan 2016

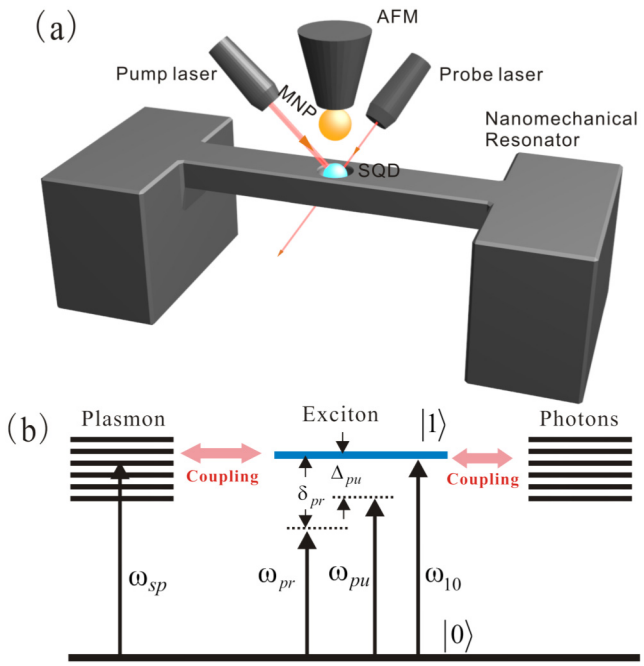

Fig. 1. (a) Schematics of a single metal nanoparticle coupled to a semiconductor quantum dot embedded in a nanomechanical resonator [34]. The system is subjected to a strong pump field and a weak probe field. (b) The level scheme of an exciton interacts with phonons and plasmons.

In a frame rotating at the pump field frequency ω_{pu}, the Hamiltonian of the MNP-SQD-NR system can be expressed as [35]

$$H = \hbar\Delta_{pu} w/2 + \hbar\omega_n b^+ b + \hbar\omega_n g w(b^+ + b)/2 - \mu(\tilde{E}_{SQD}\sigma_{10} + \tilde{E}^*_{SQD}\sigma_{01}), \qquad (1)$$

where $\Delta_{pu} = \omega_{10} - \omega_{pu}$ refers to the frequency detuning between the exciton and the pump field, $w = 2\sigma^z = \sigma_{11} - \sigma_{00}$ denotes the exciton-population inversion, ω_n denotes the mode frequency of the NR, b^+ and b represent the phonon creation operator and annihilation operator of the NR mode, respectively. We set $P = b^+ + b$. g refers to the coupling constant between the SQD and the NR. μ is the dipole moment of the exciton. $\tilde{E}_{SQD} = AE_{pu} + AE_{pr}e^{-i\delta t} + B\mu\sigma_{01}$ is the total field felt by the SQD with $A = (1 + S_\alpha\gamma(\omega)a^3/d^3)/\varepsilon_{eff}$, $B = S_\alpha^2\gamma(\omega)a^3/(\varepsilon_b\varepsilon_{eff}d^6)$, where $\varepsilon_{eff} = (2\varepsilon_b + \varepsilon_s)/(3\varepsilon_b)$, $\gamma(\omega) = (\varepsilon_m(\omega) - \varepsilon_b)/(2\varepsilon_b + \varepsilon_m(\omega))$ [36,37]. A arises from the field from the MNP which is induced by the pump field. B arises as the applied field polarizes the SQD, which in turn polarizes the MNP and then produces a field to interact with the SQD. Therefore, this can be regarded as the self-interaction of the SQD, because this coupling to the SQD depends on the polarization of the SQD [15]. $\delta = \omega_{pr} - \omega_{pu}$ is the frequency difference between the probe field and the pump field. S_α is polar factor for electric field polarization and $S_\alpha = 2$ corresponds that the polar direction is along the major axis of the system. ε_b and ε_s refer, respectively, to the dielectric constants of the background and the SQD. ε_m is the dielectric constant of the MNP [38]. $\Omega = \mu E_{pu}/\hbar$ is the Rabi frequency of the pump field and $G = \mu^2 B/\hbar$ is the feedback (self-action) parameter for the SQD.

By applying the Heisenberg equations of motion and the commutation relation $[\sigma^z, \sigma^\pm] = \pm\sigma^\pm$, $[\sigma^+, \sigma^-] = 2\sigma^z$ and $[a^+, a] = 1$, we can obtain the generalized optical Bloch equations as follows:

$$\dot{\sigma}_{01} = -\left[\Gamma_2 + i\left(\Delta_{pu} + \omega_n g P\right)\right]\sigma_{01} - iA\Omega w - \frac{i\mu}{\hbar}AE_{pr}e^{-i\delta t}w - iGw\sigma_{01}, \qquad (2)$$

#253917 Received 16 Nov 2015; revised 19 Jan 2016; accepted 22 Jan 2016; published 29 Jan 2016

$$\dot{w} = -\Gamma_1 (w+1) + 2i\Omega \left(A\sigma_{10} - A^* \sigma_{01} \right) + \frac{2i\mu}{\hbar} \left(AE_{pr} e^{-i\delta t} \sigma_{10} - A^* E_{pr}^* e^{i\delta t} \sigma_{01} \right) - 4G_I \sigma_{01} \sigma_{10}, \quad (3)$$

$$\ddot{P} + \gamma_n \dot{P} + \omega_n^2 P = -\omega_n^2 g w, \quad (4)$$

where Γ_1 and Γ_2 denote the exciton relaxation rate and the exciton dephasing rate, respectively. $G_R = \mathrm{Re}[G]$, $G_I = \mathrm{Im}[G]$, $A_R = \mathrm{Re}[A]$ and $A_I = \mathrm{Im}[A]$.

In order to solve the above equations, we make the ansatz $\sigma_{01} = \sigma_{01}^{(0)} + \sigma_{01}^{(1)} e^{-i\delta t} + \sigma_{01}^{(-1)} e^{i\delta t}$, $w = w_0 + w_1 e^{-i\delta t} + w_{-1} e^{i\delta t}$ and $P = P_0 + P_1 e^{-i\delta t} + P_{-1} e^{i\delta t}$ [39], where $\sigma_{01}^{(0)}$, w_0, P_0 are the steady-state solution of Eqs. (2)-(4). $|\sigma_{01}^{(0)}| >> |\sigma_{01}^{(1)}|,|\sigma_{01}^{(-1)}|$; $|w_0| >> |w_1|,|w_{-1}|$; $|P_0| >> |P_1|,|P_{-1}|$. We can obtain the analytical solution of $\sigma_{01}^{(-1)}$ in the appendix. The FWM signal in the steady state is given by

$$FWM = \left| \sigma_{01}^{(-1)} \Big/ \left(\mu E_{pr}^* \hbar^{-1} \Gamma_2^{-1} \right) \right|, \quad (5)$$

The exciton-population inversion in the steady state w_0 is determined by a third-order equation

$$\Gamma_1 (w_0 + 1) \left[\left(\Gamma_2 - G_I w_0 \right)^2 + \left(\Delta_{pu} - \omega_n g^2 w_0 + G_R w_0 \right)^2 \right] + 4 \left| A \right|^2 \Omega^2 \Gamma_2 w_0 = 0. \quad (6)$$

3. Results and discussion

We perform numerical calculations for a realistic coupled system including an InAs QD, a gold MNP and a GaAs NR. For the InAs QD, we take $\varepsilon_0 = 1$, $\varepsilon_s = 6\varepsilon_0$, $\mu = 40$ D, $\Gamma_1 = 0.3$ ns^{-1} and $\Gamma_2 = 0.15$ ns^{-1} [35]. For the Au MNP, $a = 5$ nm, $\varepsilon_\infty = 9.5$, $\hbar\omega_p = 8.95$ eV, $\hbar\gamma_p = 0.069$ eV [40]. For the GaAs NR, $\omega_n = 1.2$ GHz and $Q = 3 \times 10^4$ [30,31,35], where Q is the quality factor of the NR, $\gamma_n = \omega_n / Q$ is the damping rate. Before we discuss the nonlinearity of the hybrid system, we have to explain that we are only interested in a narrow frequency region near by the SQD resonance, so it is reasonable to neglect the frequency-dependence of the polarization of the MNP.

To study the FWM response of the MNP-SQD-NR system, in Fig. 2, we show how $\left| \sigma_{01}^{(-1)} / \left(\mu E_{pr}^* \hbar^{-1} \Gamma_2^{-1} \right) \right|$ changes with the probe-exciton detuning δ_{pr} for various pump field intensities I_{pu} and exciton-phonon coupling constants g as $\Delta_{pu} = 0$. As shown in Fig. 2(a), we find that the peak value of FWM signal increases as I_{pu} increases and the enhanced peak for $I_{pu} = 100$ GHz^2 is almost 10^2 times larger than that for $I_{pu} = 1$ GHz^2, which suggests that the system undergoes a linear hybrid response. The physics behind this enhancement can be understood as follow: as the pump-field intensity I_{pu} increases, the number of photons becomes increased, so the SQD will be excited more easily. In Fig. 2(b), one can see that the two sharp peaks locate at $\delta_{pr} = \pm 1.2$ GHz matching with the NR frequency ω_n very well, which provides a new way to measure the vibrational frequency of the NR [30].

To further reveal the physical properties of two sharp peaks corresponding to the resonance amplification (left peak) and absorption (right peak) of vibrational mode of the NR, in Figs. 2(c) and 2(d), we should note that, with the increase of exciton-phonon coupling constant g, the amplification peak becomes sharper and the peak intensity is enhanced significantly. More precisely, the amplification peak for $g = 0.18$ is almost three orders of magnitude times larger than that for $g = 0$. The absorption peak exhibits identical enhanced behavior. This implies that strong exciton-phonon coupling will promote the exciton-population inversion and enhance the absorption of the SQD, leading to the enhancement of FWM signal.

#253917 Received 16 Nov 2015; revised 19 Jan 2016; accepted 22 Jan 2016; published 29 Jan 2016

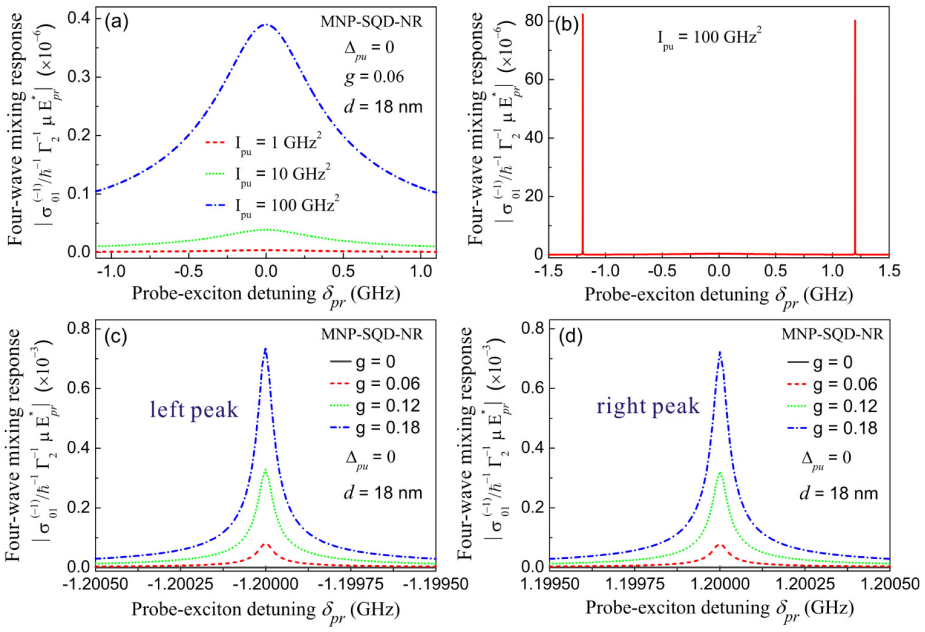

Fig. 2. (a) Four wave mixing signal as a function of probe-exciton detuning δ_{pr} for different values of pump-field intensity I_{pu}. (b) Four-wave mixing signal a as a function of δ_{pr} in a relatively wide region for I_{pu} = 100 GHz^2. The amplified left peak and right peak are shown in Figs. 2(c) and 2(d) for different coupling constants g, respectively. The other parameters used are $\Delta_{pu} = 0$ and d = 18 nm.

It is interesting to track the role of exciton-plasmon interaction in the FWM response of MNP-SQD-NR system with a given exciton-phonon coupling constant g. In Figs. 3(a-c), for $\Delta_{pu} = 0$, the magnitude of the peak of the FWM response increases as the SQD-MNP distance d increases from 12 to 18.09 nm, while the peak value decreases as d further increases from 26.33 to 30 nm. Moreover, the FWM peak reaches a maximum at d = 26.33nm, which is slightly larger than that in the SQD-NR system. It's worth mentioning that there is a bistable region $d\in$ [18.1, 26.32] nm. The results in Figs. 3(d-f) show that, as the frequency of the pump field increases ($\Delta_{pu} = -0.5\omega_n$), the bistable region becomes narrower, and the magnitude of the FWM peak is almost 2.5 times larger than that in the SQD-NR system, which is attributed to the plasmon enhancement effect. The case of $\Delta_{pu} = -1\omega_n$ in Figs. 3(g-i) is quite different. Here, the bistable region will disappear. The FWM signal is suppressed significantly in the strong exciton-plasmon interaction region with $d\in$ [12, 26.4] nm, however, a large enhancement of the FWM signal will appear in the weak exciton-plasmon interaction region with a larger d. Specifically, the magnitude of the FWM peak for d = 27.86 nm is almost 18.9 times larger than that in the SQD-NR system, and the plasmon enhancement effect for the FWM response will be weakened with a larger d. It is not difficult to find that, compared with the FWM signal in the absence of the MNP, the crossover from exciton-plasmon dominant regime to exciton-phonon dominant regime can be exhibited clearly in Figs. 3(a-i). In order to further reveal the suppression effect of the FWM response coming from the exciton-plasmon interaction, we plot the FWM spectrum with and without MNP in Fig. 3(j). The results indicate that, due to the exciton-plasmon interaction, the full width at half maximum of the FWM peak will be broadened about 2 times and the magnitude of this peak will reduce to 1/590 times than that without MNP. Such plasmon-suppressed behavior for the FWM response is compatible with that of a previous study [26]. In our system, such large suppression arises from a combination of exciton-phonon interaction and exciton-plasmon interaction.

#253917 Received 16 Nov 2015; revised 19 Jan 2016; accepted 22 Jan 2016; published 29 Jan 2016

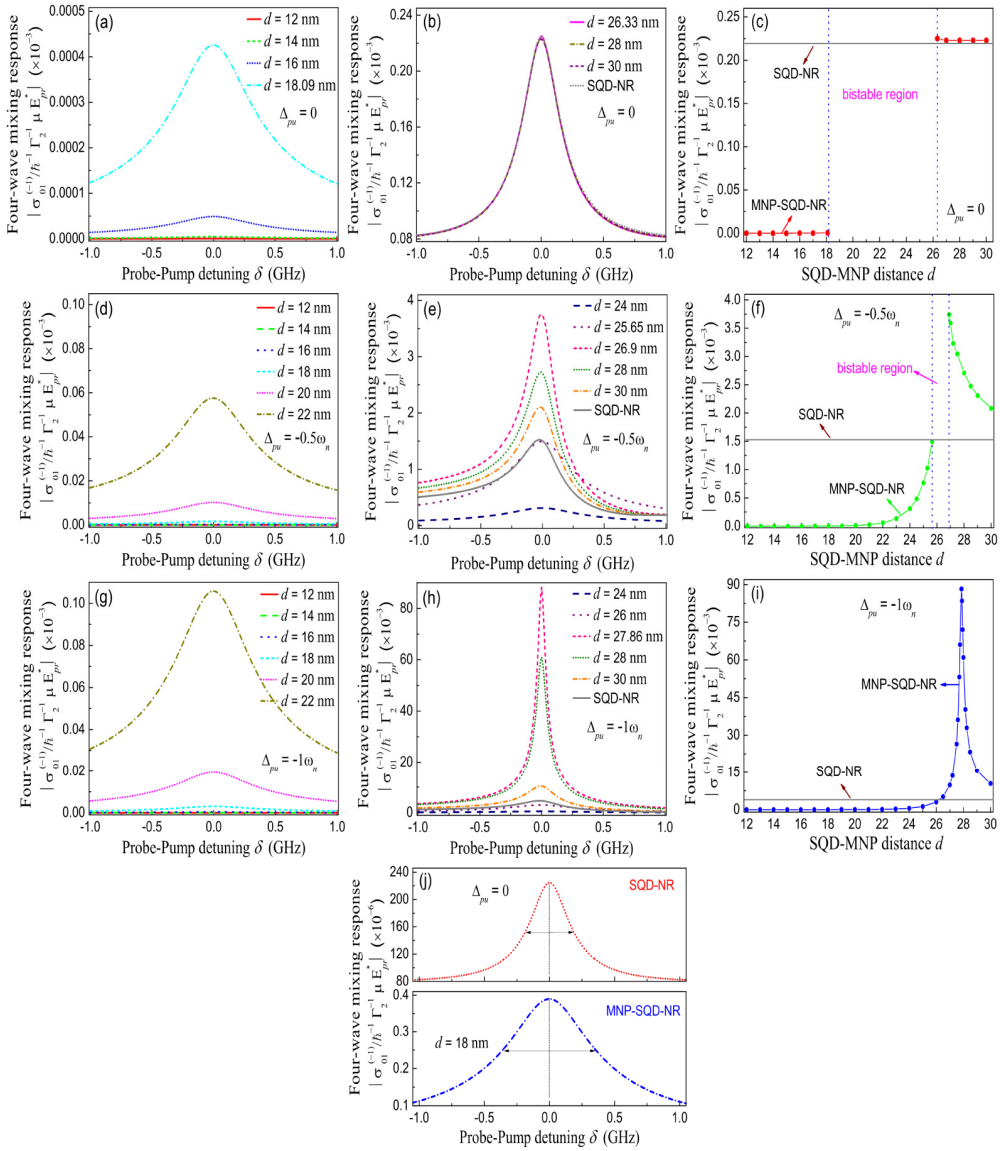

Fig. 3. Four-wave mixing signal as a function of probe-pump detuning δ for different SQD-MNP distance d when $\Delta_{pu} = 0$ (a, b), $\Delta_{pu} = -0.5\omega_n$ (d, e), $\Delta_{pu} = -1\omega_n$ (g, h). d-dependence of four-wave mixing signal when $\Delta_{pu} = 0$ (c), $\Delta_{pu} = -0.5\omega_n$ (f), $\Delta_{pu} = -1\omega_n$ (i). (j) Four-wave mixing spectrum with and without the MNP for $\Delta_{pu} = 0$. The other parameters used are g = 0.06 and $I_{pu} = 100$ GHz^2 (corresponding to $I_{pu} = 33.19$ W/cm^2).

Next, we will explore the optical bistable response of the hybrid MNP-SQD-NR system. Figure 4 shows the variation of w_0 as a function of I_{pu} for different detunings Δ_{pu}. In Fig. 4(a), we can see that, when the pump field is exactly resonant with the SQD, a prominent bistable response emerges in the hybrid system, while a strong saturable absorption appears in the SQD-NR and SQD systems. As it is well known, the exciton-population inversion will be enhanced as the pump field intensity I_{pu} increases, which induces the naked SQD and SQD-NR systems easy to reach saturation. In other word, the saturated absorption behavior will be suppressed at a certain extent when the interaction of the exciton and plasmon becomes strong. In our nanosystem, $G_R >> G_I$, which implies that the bistability mechanism is similar to that in a two-level atoms thin film, whose feedback comes from the local field [41]. In Fig.

#253917 Received 16 Nov 2015; revised 19 Jan 2016; accepted 22 Jan 2016; published 29 Jan 2016

4(b), we further study the w_0-dependent FWM response. As $\Delta_{pu} > 0$ ($\omega_{10} > \omega_{pu}$), the SQD is easy to reach resonance with the pump field under the steady-state condition $-1 < w_0 < 0$. Compared with the case of resonance ($\Delta_{pu} = 0$), as Δ_{pu} increases, the bistable thresholds move towards the direction with a smaller I_{pu}. As $\Delta_{pu} = \omega_n$, the NR begins to oscillate coherently, which leads to a Stokes-like scattering of the pump light via the exciton in the SQD. This scattering will effectively modify the bistable behavior. Moreover, there is interference between the pump field and the local field [7,15]. As I_{pu} increases, the role of the pump field in the interference will change and then influence the OB of FWM response.

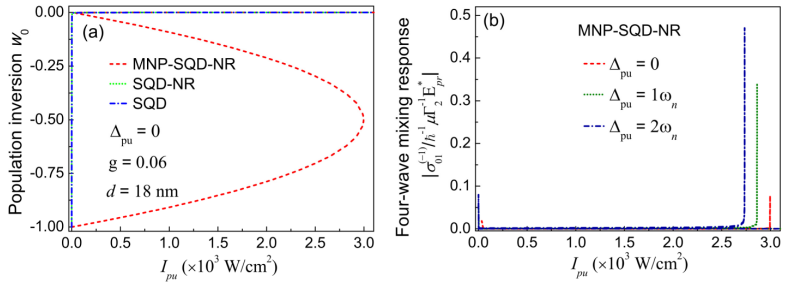

Fig. 4. (a) Steady-state population inversion w_0 as a function of I_{pu} in three different systems for $\Delta_{pu} = 0$. (b) Four-wave mixing signal $\sigma_{01}^{(-1)}/\mu E_{pr}{}^{*}\hbar^{-1}\Gamma_2^{-1}$ as a function of pump field intensity with three different detunings Δ_{pu}. The other parameters used are $g = 0.06$ and $d = 18$ nm.

Kalkbrenner et al. presented a way to attach a MNP to the end of a sharp tip of AFM [34]. We can utilize this method to detect the distance between the SQD and the MNP according to the optical response of the hybrid system. For this reason, in Fig. 5(a) we plot the curves of w_0 versus d with different detunings Δ_{pu}, I_{pu} is kept as a constant ($I_{pu} = 66.37$ W/cm^2). As $\Delta_{pu} = 0$, the bistable thresholds d_{b1} and d_{b2} ($d_{b1} < d_{b2}$) are equal to 16.03nm and 24.83nm, respectively. With the increase in Δ_{pu}, the bistable thresholds d_{b1} and d_{b2} will be reduced and moved to the direction with a stronger dipole-dipole interaction. As shown in Fig. 5(b), the FWM signals exhibit a series of sickle-shaped bistable curves. The physical origin of such behavior can be understood as follow: as d reduces, the Coulomb interaction between the SQD and the MNP will become stronger, an enhancement of the local field will arise, and the feedback of the SQD will be enhanced, promoting the occurrence of bistability. In Figs. 4(b) and 5(b), the hysteresis loops are difficult to be observed, because the upper and lower branches of bistable curves almost overlap together. Moreover, our system can act as a quantum switch by dynamically tuning the distance between the SQD and the MNP. For $d_{b1} \le d \le d_{b2}$, the quantum switch is turned on, and the bistable effect will occur; for $d \le d_{b1}$ or $d \ge d_{b2}$, the switch is turned off, and the bistable effect will disappear. These effects provide a novel way to detect the spacing between two nanoparticles.

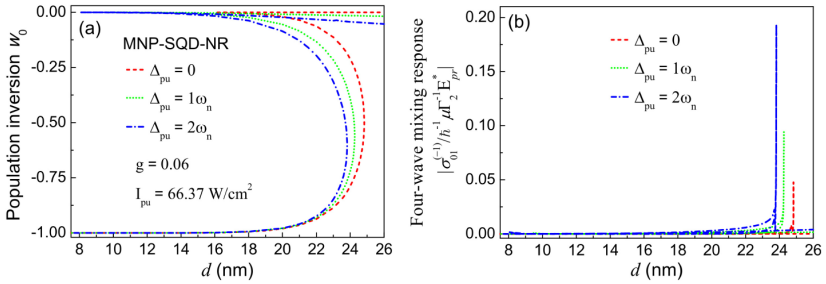

Fig. 5. Steady-state population inversion w_0 (a) and four-wave mixing signal $\sigma_{01}^{(-1)}/\mu E_{pr}{}^{*}\hbar^{-1}\Gamma_2^{-1}$ (b) as a function of the SQD-MNP distance d with three different detunings Δ_{pu}. The other parameters used are $g = 0.06$ and $I_{pu} = 66.38$ W/cm^2 (corresponding to $I_{pu} = 200$ GHz^2).

#253917 Received 16 Nov 2015; revised 19 Jan 2016; accepted 22 Jan 2016; published 29 Jan 2016

To clarify the impact of the exciton-phonon interaction on the bistable FWM response, in Fig. 6, we study the dependence of FWM response on the exciton-phonon coupling constant g. We note that the numerical solutions of Eq. (6) change slightly with g. The magnitude of g depends strongly on the material and structure of NR [35]. For a constant pumping I_{pu} and a fixed spacing d, a bistable behavior appears in the FWM signal. When g increases, the lower branch of the bistable curve lies near the line $w_0 = -1$; when g sweeps back, the upper branch of the bistable curve stays near the line $w_0 = 0$ (see inset in Fig. 6). The physics behind the bistable FWM response discussed in the previous section can be explained by the feedback providing by the exciton-plasmon and exciton-phonon interactions. These interactions result in a self-action of the SQD via the MNP and the NR. The feedback effect can be tuned by adjusting the SQD-MNP distance, the pumping intensity and nanostructural parameters.

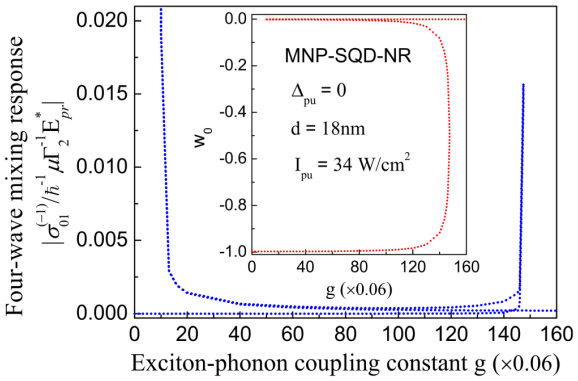

Fig. 6. Four-wave mixing signal $\sigma_{01}^{(-1)}/\mu E_{pr}$*$\hbar^{-1}\Gamma_2^{-1}$ as a function of the exciton-phonon coupling constant g. The other parameters used are $\Delta_{pu} = 0$, $d = 18$ nm, and $I_{pu} = 34$ W/cm^2. The inset shows the g-dependence of steady-state population inversion w_0.

4. Conclusion

We deduced theoretically the analytical formulas of the FWM signal by means of the method of density matrix, and explored the FWM and OB in the hybrid MNP-SQD-NR system. We illustrated that the FWM signal can be enhanced dramatically due to the exciton-phonon interaction, and the FWM signal can also be suppressed and broadened arising from the exciton-plasmon interaction. We also showed that the bistable FWM response can be realized by adjusting the SQD-MNP distance and the pumping intensity. For a given pumping constant and a fixed SQD-MNP distance, the enhanced exciton-phonon interaction can promote the occurrence of bistability. Our findings provide a feasible way to detect the spacing between the SQD and the MNP in terms of the dynamical evolution of the bistable thresholds, and hold promise for developing quantum switches and nanoscale rulers.

5. Appendix: the solution of the optical Bloch equations

In order to solve the equations (2)-(4), we make the ansatz $\sigma_{01} = \sigma_{01}^{(0)} + \sigma_{01}^{(1)}e^{-i\delta t} + \sigma_{01}^{(-1)}e^{i\delta t}$, $w = w_0 + w_1e^{-i\delta t} + w_{-1}e^{i\delta t}$ and $P = P_0 + P_1e^{-i\delta t} + P_{-1}e^{i\delta t}$ [35], where $\sigma_{01}^{(0)}$, w_0, P_0 are the steady-state solution of Eqs. (2)-(4). $|\sigma_{01}^{(0)}| >> |\sigma_{01}^{(1)}|,|\sigma_{01}^{(-1)}|$; $|w_0| >> |w_1|,|w_{-1}|$; $|P_0| >> |P_1|,|P_{-1}|$. On substituting these expressions into equations (2)-(4), and working to the lowest order in E_{pr}, but to all orders in E_{pu}, we can obtain in the steady state

$$-\left(\Gamma_2 + i\Delta_{pu}\right)\sigma_{01}^{(0)} - i\omega_n g P_0\sigma_{01}^{(0)} - iA\Omega w_0 - iGw_0\sigma_{01}^{(0)} = 0, \tag{7}$$

$$-\left(\Gamma_2 + i\Delta_{pu}\right)\sigma_{01}^{(1)} - i\omega_n g\left(P_0\sigma_{01}^{(1)} + P_1\sigma_{01}^{(0)}\right) - iA\Omega w_1 - \frac{i\mu}{\hbar}AE_{pr}w_0 - iG\left(w_0\sigma_{01}^{(1)} + w_1\sigma_{01}^{(0)}\right) = -i\delta\sigma_{01}^{(1)}, \tag{8}$$

#253917 Received 16 Nov 2015; revised 19 Jan 2016; accepted 22 Jan 2016; published 29 Jan 2016

$$-\left(\Gamma_2+i\Delta_{pu}\right)\sigma_{01}^{(-1)}-i\omega_n g\left(P_0\sigma_{01}^{(-1)}+P_{-1}\sigma_{01}^{(0)}\right)-iA\Omega w_{-1}-iG\left(w_0\sigma_{01}^{(-1)}+w_{-1}\sigma_{01}^{(0)}\right)=i\delta\sigma_{01}^{(-1)}, \tag{9}$$

$$-\Gamma_1\left(w_0+1\right)+2i\Omega\left(A\sigma_{01}^{(0)*}-A^*\sigma_{01}^{(0)}\right)-4G_I\sigma_{01}^{(0)}\sigma_{01}^{(0)*}=0, \tag{10}$$

$$-\Gamma_1 w_1+2i\Omega\left(A\sigma_{01}^{(-1)*}-A^*\sigma_{01}^{(1)}\right)+\frac{2i\mu}{\hbar}AE_{pr}\sigma_{01}^{(0)*}-4G_I\left(\sigma_{01}^{(0)}\sigma_{01}^{(-1)*}+\sigma_{01}^{(0)*}\sigma_{01}^{(1)}\right)=-i\delta w_1, \tag{11}$$

$$-\Gamma_1 w_{-1}+2i\Omega\left(A\sigma_{01}^{(1)*}-A^*\sigma_{01}^{(-1)}\right)-\frac{2i\mu}{\hbar}A^*E_{pr}^*\sigma_{01}^{(0)}-4G_I\left(\sigma_{01}^{(0)}\sigma_{01}^{(1)*}+\sigma_{01}^{(0)*}\sigma_{01}^{(-1)}\right)=i\delta w_{-1}, \tag{12}$$

$$P_0=-gw_0, \tag{13}$$

$$P_1=\frac{\omega_n^2 g}{\delta^2+i\gamma_n\delta-\omega_n^2}w_1=g\zeta w_1, \tag{14}$$

$$P_{-1}=g\zeta^* w_{-1}, \tag{15}$$

By solving the equations (7)-(15), we can obtain the solution for $\sigma_{01}^{(0)}$, w_0, P_0, $\sigma_{01}^{(1)}$, w_1, P_1, $\sigma_{01}^{(-1)}$, w_{-1}, P_{-1} in the appendix. The four-wave mixing signal is given by

$$FWM=\left|\sigma_{01}^{(-1)}\Big/\left(\mu E_{pr}^*\hbar^{-1}\Gamma_2^{-1}\right)\right|=\hbar\Gamma_2\left(D_1w_0-D_2\sigma_{01}^{(0)}\right)\Big/\mu D_0, \tag{16}$$

where

$$\sigma_{01}^{(0)}=\left[\left(A_I-iA_R\right)\Omega w_0\right]/[(\Gamma_2-G_I w_0)+i(\Delta_{pu}-\omega_n g^2 w_0+G_R w_0)].$$

$$D_0=C_1C_5C_7-C_2C_4C_7+C_1C_6,$$

$$D_1=C_{30}C_4,$$

$$D_2=C_1C_{30},$$

$$C_1=(\Gamma_2-G_I w_0)+i(\delta-\Delta_{pu}+\omega_n g^2 w_0-G_R w_0),$$

$$C_2=\left(A_I+iA_R\right)\Omega+\left(G_I+iG_R+i\omega_n g^2\zeta*\right)\sigma_{01}^{(0)*},$$

$$C_3=C_{30}E_{pr}*,$$

$$C_{30}=\mu\left(A_I+iA_R\right)/\mathrm{h},$$

$$C_4=-\left(4G_I\sigma_{01}^{(0)}+2A_I\Omega\right)+2iA_R\Omega,$$

$$C_5=i\delta+\Gamma_1,$$

$$C_6=2A_I\Omega+4G_I\sigma_{01}^{(0)*}+2iA_R\Omega,$$

$$C_7=[\Gamma_2+i(\delta+\Delta_{pu}+Gw_0-\omega_n g^2 w_0)]/\left[\left(A_I\Omega+G_I\sigma_{01}^{(0)}\right)-i\left(A_R\Omega+G_R\sigma_{01}^{(0)}+\omega_n g^2\zeta*\sigma_{01}^{(0)}\right)\right],$$

$$\zeta=\omega_n^2/(\delta^2+i\gamma_n\delta-\omega_n^2).$$

Acknowledgments

We would like to thank Hua Zhang, Jia-Guang Chen, Zheng-Feng Li, and Guo-Fan Quan for their helpful discussions. This work was supported by the National Natural Science Foundation of China (NSFC) (Grant Nos. 11404410 and 11174372), the Hunan Provincial Natural Science Foundation (Grant No. 14JJ3116), the Project of Innovation-driven Plan in Central South University (Grant No. 2015CXS1035) and the Foundation of Talent Introduction of Central South University of Forestry and Technology (Grant No. 104-0260).